ISSN: 2230-9926

Available online at http://www.journalijdr.com

IJDR

International Journal of Development Research
Vol. 5, Issue, 10, pp. 5725-5762, October, 2015

International Journal of
DEVELOPMENT RESEARCH

Full Length Research Article

STRUCTURAL AND ELECTRICAL BEHAVIOR OF TIN DOPED $Ba_{0.6}Sr_{0.4}TiO_3$ THIN FILMS

Eswaramoorthi, V. and *Victor Williams, R.

Department of Physics, St. Joseph's College (Autonomous), Tiruchirappalli 620002, India

ARTICLE INFO

Article History:

Received 29th July, 2015
Received in revised form
17th August, 2015
Accepted 19th September, 2015
Published online 31st October, 2015

Key Words:

BST, Sol-gel,
Dielectric properties,
Ferroelectricity.

ABSTRACT

(Ba, Sr)TiO_3 (BST) thin films doped with Tin were coated by sol-gel method on quartz and stainless steel substrates. The results of X-ray diffraction and FE-SEM analysis had shown that the grain size of BST thin films decreases with dopant concentration. Dielectric properties were investigated as a function of frequency. The dielectric constant and dielectric loss of BST thin films decreases with dopant concentration and was explained by electro negativity and oxygen vacancy factors. The retendivity of the specimen decreases while the coercive force increases with dopant concentration.

INTRODUCTION

The ferroelectric materials have been intensively studied for memory device applications due to their unique properties. The infrared thermal imaging system is used in civil and military applications. The traditional photon type infrared focal plane arrays (FPA) need to be cooled at a temperature of about 77K that involves highly intricate mechanical cryogenic system and high cost (Piotrowski *et al*., 1998). The uncooled infrared focal plane arrays (UFPA) increases the life time of the system and is also cost effective (Liu *et al*., 2003). The ferroelectric barium strontium titanate (BST) thin films have attracted attention for their potential application in ferroelectric microbolometers as UFPA due to their high dielectric constant, low loss tangent and high breakdown strength (Lee *et al*., 1999; Cheng *et al*., 1999; Zhang *et al*., 2002). It has also attracted much interest because of its potential applications in devices such as DRAM (Kumar *et al*., 2005), thin film capacitors (Kurihara *et al*., 2004) and actuators (Uchino 1994). The dopants modify the properties of BST thin films. According to previous investigations (Joshi *et al*., 2000; Cha *et al*., 1999) the electrical properties of BST thin films were affected by the deposition method, film composition microstructure, film thickness and type of dopant.

Corresponding author: Victor Williams, R.
Department of Physics, St. Joseph's College (Autonomous), Tiruchirappalli 620002, India

The dopants occupy the B site in ABO_3 perovskite structure (Fe^{2+}, Fe^{3+}, Co^{2+}, Mn^{2+}, Cr^{3+} and Sc^{3+}) to reduce the leakage current density and dielectric loss (Kim *et al*., 2005; Yoon *et al*., 2001; Chen *et al*., 2001). The novelty of the present work includes the investigation of structural and electrical behavior of Tin doped BST thin films at different concentrations on quartz and stainless steel substrates by sol-gel process.

Experimental Details

Tin doped BST thin films were prepared by sol-gel method using barium acetate, strontium acetate, titanium IV butoxide and dibutyl tin IV oxide as precursor solutions. Glacial acetic acid and acetyl acetone were used as solvent and stabilizing agent respectively. Barium acetate and strontium acetate in a mole ratio of 60:40 was dissolved in heated glacial acetic acid. Dibutyl tin IV oxide (as a dopant precursor with concentrations of 1%, 2% and 4%) was dissolved in a glacial acetic acid and added to the solution by drops with constant stirring at room temperature. After 30 min a few drops of acetyl acetone was added to stabilize the solution. Titanium IV butoxide was added to the solution in drops and stirred for 90 min. The colorless solution turned into pale yellow and the viscosity of the solution was increased gradually due to cross linking reaction. After 63 hours the solution attained a suitable viscosity for coating. The gelation time was found to be 64 hrs. For the fabrication of Tin doped BST thin films the sol was spun onto quartz and stainless steel substrate at 5500 rpm

for 60 s. The coated films were kept in a hot plate for 400°C for 30 min to remove the organic volatiles. The prebaked films were annealed for 30 min under 800°C to obtain crystallization. The thickness of the film was measured using the profilometer (Mitutoyo SJ 301) and FE-SEM. The texture of the film was analyzed by X-ray diffractometer (XPERT-PRO). FE-SEM (FEI quanta-250) explored the surface morphology of the films. The dielectric properties were carried out using a metal-insulator-metal (MIM) capacitor cell. For this measurement Aluminum (1cm X 1cm) was used as top electrode. Capacitance-Voltage, dielectric constant and dielectric loss measurements were carried out using LCR meter.

RESULTS AND DISCUSSION

X-ray diffraction (XRD) analysis

Figure 1(a) shows the X-ray diffraction pattern of Tin doped BST thin films coated onto a quartz substrate with various dopant concentrations (1-4%) annealed at 800°C for about 30 min. The characteristics peaks in the XRD pattern confirm the presence of BST material (JCPDS Card no: 34-0411).

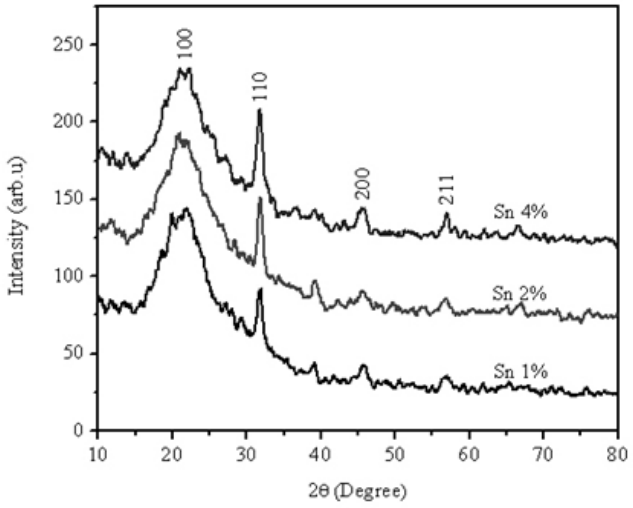

Fig. 1(a). X-ray diffraction of BST thin films for different Tin contents (1 – 4%)

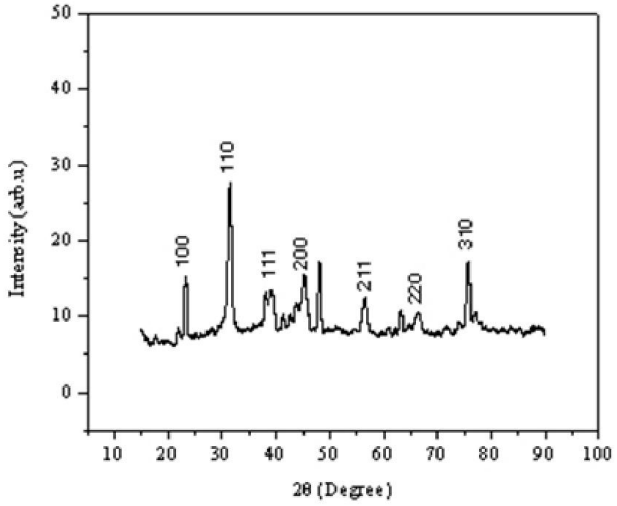

Fig. 1(b). X-ray diffraction of BST thin films on Stainless steel substrate

Figure 1 (b) shows the characteristic peaks for the BST films without the effect of stainless steel substrate.

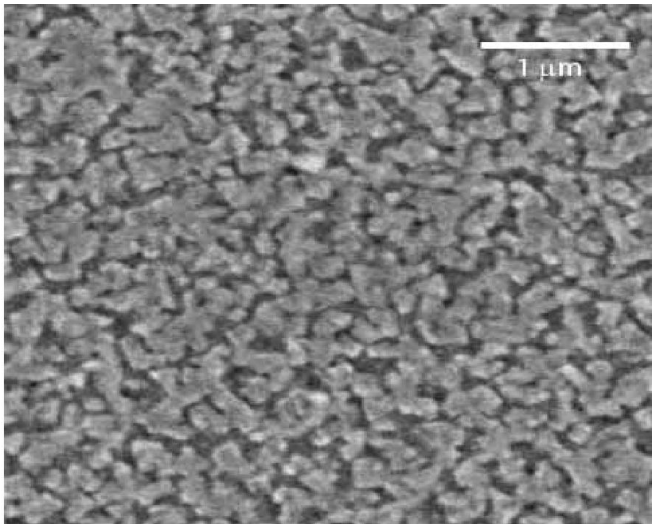

Fig. 2(a). FE-SEM image of 1% Tin doped BST thin films

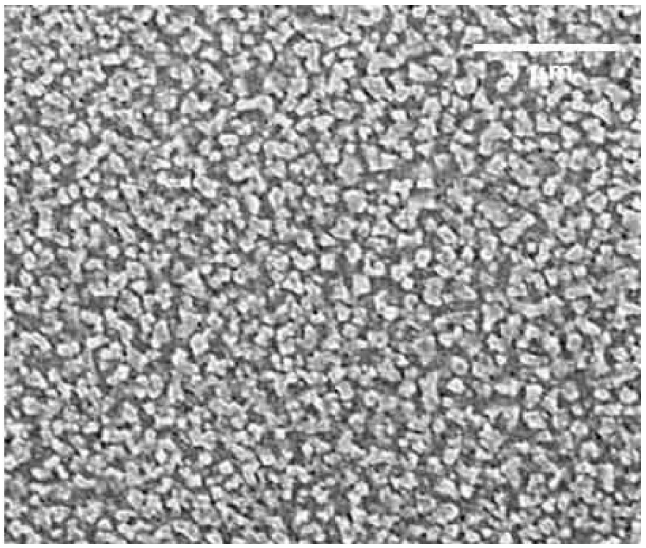

Fig. 2(b). FE-SEM image of 2% Tin doped BST thin films

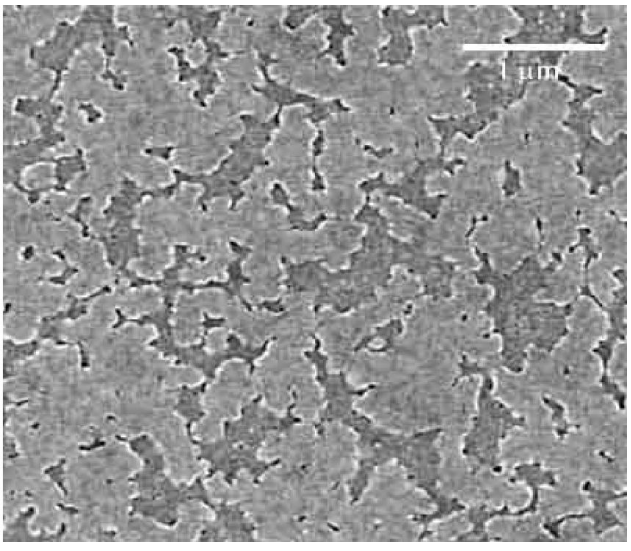

Fig. 2(c). FE-SEM image of 4% Tin doped BST thin films

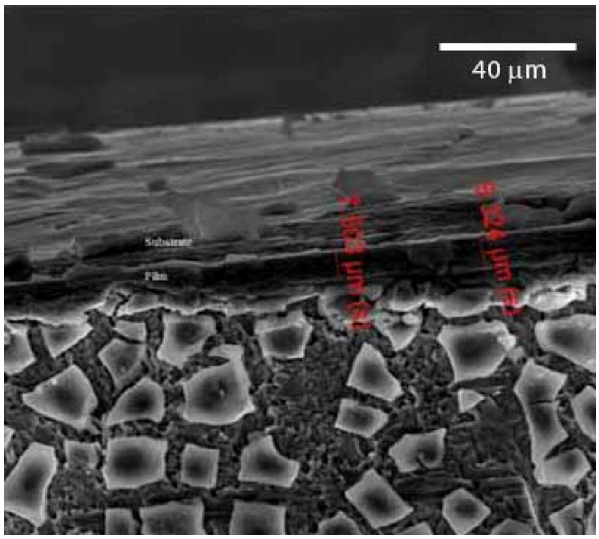

Fig. 3(a) . Cross sectional FE-SEM image of 1% Tin doped BST thin films

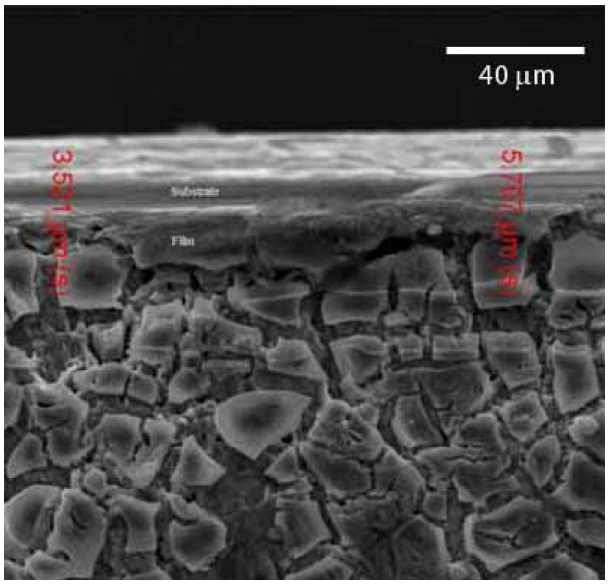

Fig. 3(b). Cross sectional FE-SEM image of 2% Tin doped BST thin films

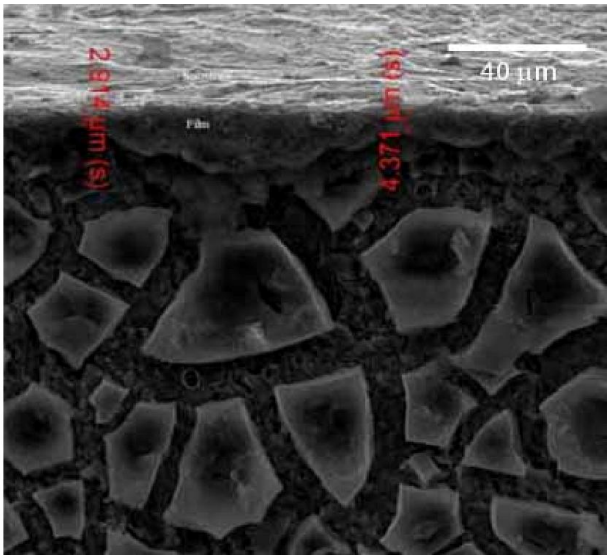

Fig. 3(c). Cross sectional FE-SEM image of 4% Tin doped BST thin films

The XRD pattern indicates that the films are polycrystalline suggesting a complete perovskite phase formation with the absence of secondary phase. The absence of the secondary phase (derivatives of tin oxide) increases the dielectric constant and reduces the leakage current density [11]. The XRD pattern shows that the increased dopant concentration (1 - 4%) leads to increase in intensity of diffraction peaks. XRD pattern reveals the improvement in crystalline natureas the Tin is replaced with Ti. The lattice constant (a) of the samples are calculated from 2θ values of the XRD pattern using Check Cell software and manually through Bragg's law (Table 1). The (110) peak shifts towards left in the XRD pattern, which is due to the variation in the lattice constant. The peak positions and full width half maximum values of all the films are listed in Table 2. Using these values, the grain size was calculated using Scherrer formula and listed in Table 1.

$$D = \frac{0.9\lambda}{\beta \cos\theta} \qquad (1)$$

The variation in the lattice parameters of Tin doped BST thin films with change in dopant concentration may be attributed to the change in ionic radius. The ionic radii of Ba^{2+}, Sr^{2+}, Ti^{4+} and Sn^{4+} are 1.34, 1.12, 0.68 and 0.69 Å respectively. Hence the ionic radius of Sn^{4+} is approximately equal to that of Ti^{4+} and hence Tin can be easily diffused into the lattice and may substitute on B site atom in ABO_3 perovskite structure. The increased value of lattice parameters indicates that Tin ion substitutes the B site of ABO_3 structure (Hu *et al*., 2008).

Morphology and Compositional analysis

The surface morphologies of the Tin doped BST thin films are evaluated using FE-SEM as shown in Fig 2 (a-c). The films exhibit crack-free uniform surface. The addition of Tin to the BST lattice decreases the grain size of the crystallized films. The decreasing grain size due to the replacement of Ti by Tin leads to slower diffusion of Sn^{4+} in BST lattice. This causes the effect in thickness of doped BST thin films with different doping concentration. The thickness of the films decreases with increasing concentration from 1 to 4%. In this Ti^{4+} has smaller ionic radius than Tin. The effect of doping on grain size is usually interpreted in terms of dopant solubility and distribution of doping ions between the surface and interior parts of the grain. The segregation of impurity ions at grain boundaries can impede the grain growth (Hu *et al*., 2008). Thicknesses of the samples are measured using FE-SEM and cross verified by profilometer (Table 3). The cross sectional FE-SEM view of the samples kept in a slanding positions are shown in Fig 3(a-c).The composition of the film was analyzed using energy dispersive X-ray spectrum (EDX) (Fig. 4(a), 4(b) and 4(c)). The EDX spectra of tin doped BST thin films, confirms the presence of barium, strontium, titanium and tin and the data are presented in Table 4.

Ferroelectric properties

The polarization and electric field (P-E) characteristics are measured at room temperature for the samples coated on stainless steel substrates (2cm x 1cm) and are shown in Fig 5. The P-E characteristics exhibit hysteresis loops that indicate

the ferroelectric behavior of Tin doped BST thin films. Due to the decrease of grain size the remanent polarization decreases with increase of Tin doping.

It may be attributed to the oxygen vacancy pinned at BST thin films as Tin atom finds it difficult to move near the lattice's center of gravity (Hu *et al*., 2007).

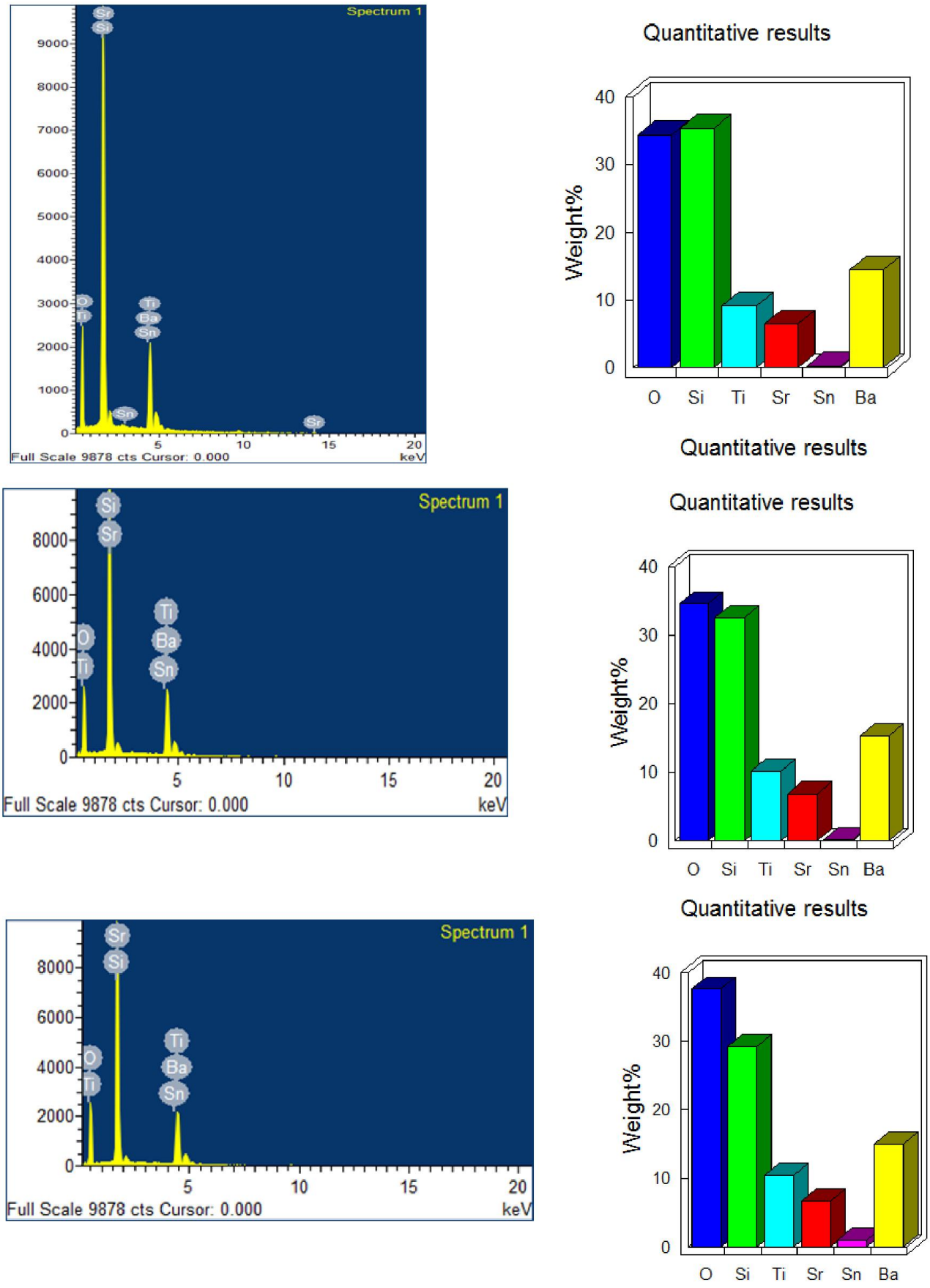

Fig. 4. EDX spectrum of 1, 2, 4 % Sn doped BST thin films

The remanent polarization (P_r) values and the Coercive field (E_c) of the Tin doped BST thin films with different dopant concentrations are +0.163, +0.139, +0.102 μC/cm^2 and +1.384, +1.796, +2.934 KV/cm respectively. The coercive field (E_c) increases with decrease in thickness of the film (Damjanovic 1998).

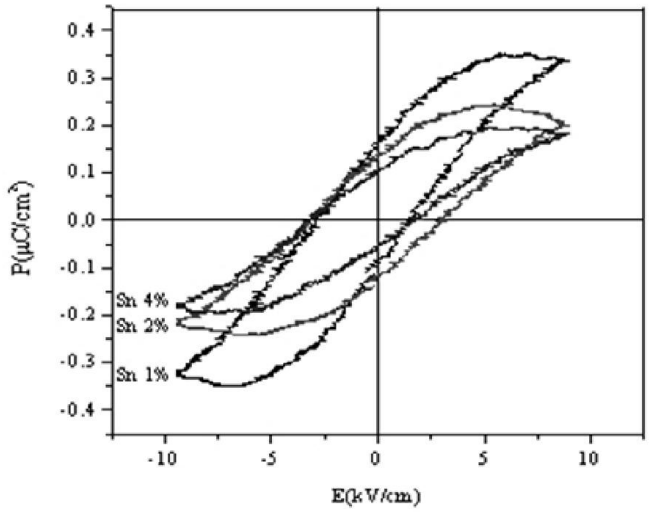

Fig. 5. The P – E hysteresis loops of BST thin films for different Tin contents (Stainless steel substrates)

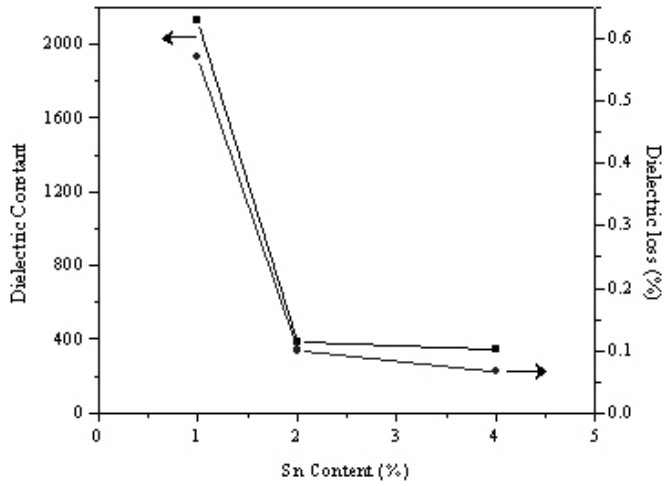

Fig. 6. Dielectric constant and dielectric loss of BST thin films as a function of Tin content

Dielectric properties

The dielectric constant of Tin doped BST thin films at a frequency of 100 KHz are as shown in Fig.6. The dielectric constant varies with the applied voltage (Fig.7). The dielectric constant of the film is strongly affected by the microstructure and grain size. A larger grain size results in more polarization. The polarization of the material is directly proportional to the dielectric constant of the material. The grain size of the films decreases with the dopant concentration, results in lowering the dielectric constant (Table 1). It is well known that the dielectric properties of the ferroelectric materials depend on the domain wall oscillation (Hu *et al*., 2007) and electronegativity factor (Wang *et al*., 2004).

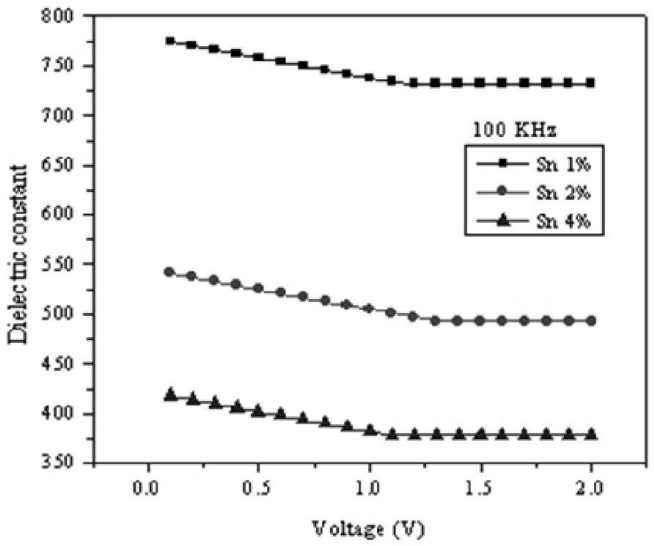

Fig. 7. Dielectric constant of BST thin films as a function of dc bias

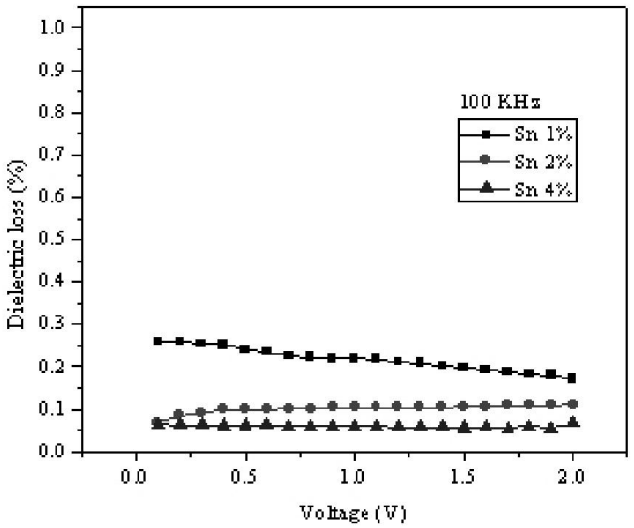

Fig. 8. Dielectric loss of BST thin films as a function of dc bias

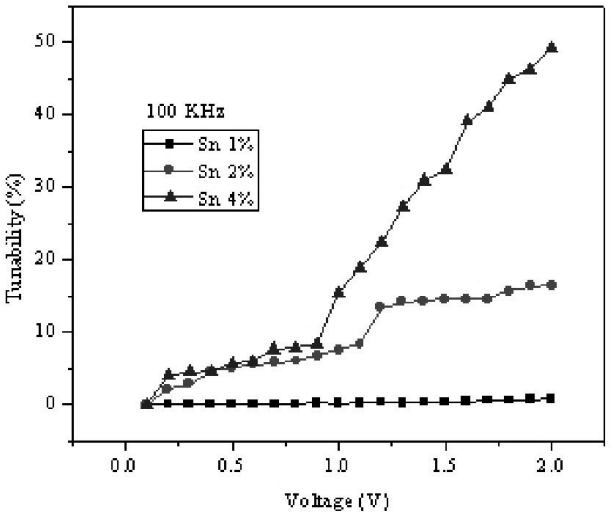

Fig. 9. Tunability of BST thin films as a function of dc bias

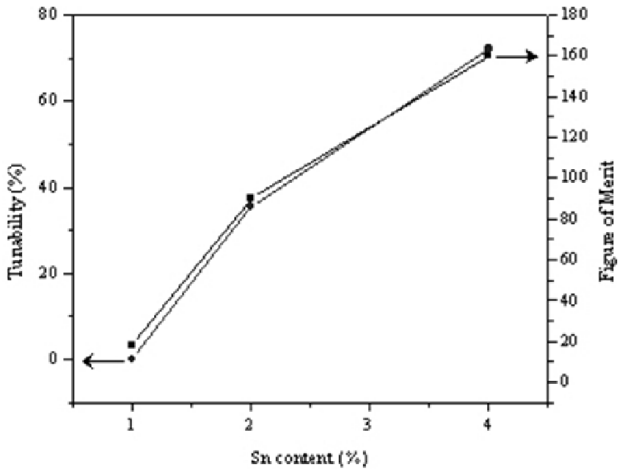

Fig. 10. Tunability and FOM of BST thin films as a function of Tin concentration

The decrease in dielectric constant may be due to the segregation effect that has been confirmed from XRD or the oxygen vacancy present on the surface of the film which may act as pinning centers. The electro negativity of Tin is greater than Ti that reduces the polarization of BST thin films, causing the decrease of dielectric constant. The dielectric loss of the Tin doped BST thin films at a frequency of 100 KHz are as shown in Fig.6 and Fig.8. The dielectric loss originates from two mechanisms: resistive loss and relaxation loss. In resistive loss mechanism (Tsai *et al*., 1997), the dielectric loss is mainly due to mobile charges in the film such as oxygen vacancy. The electrovalence of Tin ion is changeable, which is capable of forming +2 and +4 ions. This occurs both in solid and liquid state (Chambers *et al*., 1975). The *s* and *p* electrons are involved in the oxidation state of +4. The *p* electrons involve only in the oxidation state +2 where as two *s* electrons are retained as inert pair. As Tin ion changes from +4 to +3 (or +2), the oxygen vacancies are pinned.

Table 1. The 2θ (110) values of reflection peaks, the corresponding lattice parameters and the grain sizes of Tin doped BST thin films

Films	1% Tin doped BST	2% Tin doped BST	4% Tin doped BST
2θ (110)	31.81	31.82	31.76
a (Å)(software)	3.967	3.974	3.982
a (Å)(Bragg's law)	3.970	3.973	3.981
Grain size (nm)	36.44	26.69	14.41

Table 2. The peak positions and FWHM values of all the film

Films	Peak positions(2θ)	FWHM values	Height [cts]	d-spacing [Å]	Rel. Int. [%]
1% Tin doped BST	21.87	6.0	44	4.06136	100.00
	31.81	0.4	41	2.81076	92.17
	39.10	0.0	03	2.30149	07.60
	45.71	1.1	08	1.98327	19.29
	56.80	1.2	06	1.61959	14.11
2% Tin doped BST	21.96	5.3	36	4.04435	90.42
	31.82	0.5	40	2.80995	100.00
	39.20	0.7	06	2.29430	14.38
	56.70	1.0	06	1.62338	15.92
4% Tin doped BST	31.76	1.0	42	2.81500	100.00
	46.00	1.0	10	1.97947	23.76
	57.01	0.2	18	1.61407	42.27

Table 3. Thickness values of Tin doped thin films with various concentrations measured from FE-SEM and Profilometer

Samples	Thickness	
	FE-SEM (μm)	Profilometer (μm)
1% Tin doped BST	7.5 – 9.3	8.1
2% Tin doped BST	3.5 – 5.7	5.5
4% Tin doped BST	2.9 – 4.3	4.2

Table 4. Compositional analysis of Ga doped BST thin films at various doping concentrations

Sample code	Sn doped BST thin films		
	1 %	2 %	4 %
Element	Atomic %	Atomic %	Atomic %
O K	56.88	57.98	61.79
Si K	33.31	31.12	27.40
Ti K	5.03	5.73	5.70
Sn K	0.05	0.06	0.21
Sr L	1.95	2.11	2.03
Ba L	2.77	3.01	2.87

This is the reason for decrease in dielectric loss.

$$O^{2-} \Rightarrow \frac{1}{2} O_2 + 2e^-$$

$$Sn^{4+} + e^- \rightarrow Sn^{3+}$$

$$Sn^{3+} + e^- \rightarrow Sn^{2+}$$

The lower dielectric loss can be attributed to the dopants acting as a donor in the BST structure suppressing the inherent vacancy concentration, prohibiting the formation of charge carriers, that leads to decrease in polarization. The dopant Tin decreases the dielectric loss of the films and has obvious influence on dielectric constant similar to the other dopants (Kim *et al*., 2005; Dimos *et al*., 1997).

Tunability of the capacitance

The tunability of the capacitance is calculated using the relation $\frac{C_{max} - C_{min}}{C_{min}} \times 100$.

C_{max} denotes the capacitance value for zero bias fields and C_{min} denotes the capacitance value for the applied field (Liang *et al*., 2005). Fig.9 shows the variation of tunability with applied voltage. The variation of tunability of Tin doped BST thin films with different dopant concentration are shown in Fig.10. The tunability is increased with dopant concentration (Hu *et al*., 2008). The values of tunability on stainless steel substrates are 3.4, 37.3 and 70.6%. To the best of our knowledge 76% is the highest reported value for $BaTiO_3$ thin films doped with Tin by sol-gel on Pt-silicon substrates (Mascot *et al*., 2011). The increase in tunability is due to the smaller stress present in larger grains. The reduction of oxygen vacancies due to Tin doping improves the dielectric behavior of BST thin films (Kim *et al*., 2006).

The Figure of Merit (FOM) is a parameter used to characterize correlations between tunability and dielectric loss and it is defined as $\text{FOM} = \frac{\%\ \text{tunability}}{\%\ \text{dielectricloss}}$ This expression denotes a tunable microwave circuit cannot take full advantage of high tunability if the dielectric loss is too high. Fig. 10 shows that FOM increases with increasing dopant concentration.

Conclusion

The sol-gel routed Tin doped BST thin films were coated on quartz and stainless steel substrates. XRD studies on deposited thin films exhibited polycrystalline nature in cubic crystal system with smaller grain size. FE-SEM micrographs confirmed the crack free and uniform surface of the film. The dielectric constant and dielectric loss decreased relative to undoped film. The tunability of the film changed with different concentrations of Tin. The figure of merit of tunability changed with increase in dopant concentration. The P – E characteristics graph showed the ferroelectric behavior of the films. The remanent polarization (P_r) and the coercive field (E_c) of thin films were +0.163, +0.139, +0.102 μC/cm^2 and +1.384, +1.796, +2.934 KV/cm respectively. The tin doped BST thin films coated over the stainless steel substrates are suitable for applications in voltage tunable transducers and thermal sensors.

REFERENCES

Cha, S. Y, Jang, B. T and Lee, H. C. 1999. Effects of Ir Electrodes on the Dielectric Constants of $Ba_{0.5}Sr_{0.5}TiO_3$ Films**,** *Japanese J. Appl. Phys.* 38, pp.L49-L51.

Chambers, C., Holiday, A. K. 1975. Modern Inorganic Chemistry, Butterworth & Co Ltd, London.

Chen S. Y, Wang H. W and Huang L. C. 2001. Electrical Properties of Mg/La, Mg/Nb Co-Doped $(Ba_{0.7}Sr_{0.3})TiO_3$ Thin Films Prepared by Metallo-Organic Deposition Method, *Japanese J. Appl. Phys.* 40, pp.4974-4978.

Cheng, J. G, Meng, X. J, Tang, J, Guo, S. L. Chu, J. H. 1999. Pyroelectric $Ba_{0.8}Sr_{0.2}TiO_3$ thin films derived from a 0.05 M solution precursor by sol–gel processing, *Appl. Phys. Lett.* 75, pp.3402-3404.

Damjanovic, D. 1998. Ferroelectric, dielectric and piezoelectric properties of ferroelectric thin films and ceramics, *Rep. Prog. Phys*. 61, pp.1267-1324.

Dimos, D., Raymond, M. V, Schwartz, R. W, Alshareef, H. N and Mueller C. H. 1997. Tunability and Calculation of the Dielectric Constant of Capacitor Structures with Interdigital Electrodes, *J. Electro. Ceram*. 1, pp.145-1

Hu, W, Yang, C. and Zhang, W. 2008. Fabrication and characteristics of La, Cd and Sn doped BST thin films by sol–gel method, *J. Mater. Sci*: Mater electron. 19, pp.1197-1201.

Hu, W., Yang, C., Liu, X., He, W. and Tang, X. 2008. Characterization of Sn-doped BST thin films on $LaNiO_3$–coated Si substrate, *J. Mater. Sci:Mater electron*. 19, pp. 61-66.

Hu, W., Dong, D., Liu, X., He, W. and Tang, X. 2007. Sol–gel preparation and characterization of $Ba_{0.65}Sr_{0.35}(Ti_{0.95}Sn_{0.05})O_3$ thin films, Integrated Ferroelectrics, 92, pp.135-146.

Joshi, P. C. and Cole, M. W. 2000. Mg-doped $Ba_{0.6}Sr_{0.4}TiO_3$ thin films for tunable microwave applications, Appl. Phys. Lett. 77, pp.289-291.

Kim, K. T and Kim, C. I. 2005. The effect of Cr doping on the micro structural and dielectric properties of $(Ba_{0.6}Sr_{0.4})TiO_3$ thin films, *Thin Solid Films*. 472, pp.26-30.

Kim, K. T and Kim, C. I. 2006. Electrical and dielectric properties of Ce-doped $Ba_{0.6}Sr_{0.4}TiO_3$ thin films, *Surf. Coat. Technol.* 200, pp.4708-4712.

Kumar, A. and Manavalan, S. G. 2005. Characterization of barium strontium titan ate thin films for tunable microwave and DRAM applications, *Surf. Coat. Technol.* 198, pp.406-413.

Kurihara, K, Shioga, T. and Baniecki, J. D. 2004. Electrical properties of low-inductance barium strontium titanate thin film decoupling capacitors, *J. European Ceram. Society*. 24, pp.1873-1876.

Lee, J. S., Park, J. S, Kim, J. S, Lee, J. H, Lee, Y. H, Hahn, S. R. 1999. Preparation of $(Ba,Sr)TiO_3$ Thin Films with High Pyroelectric Coefficients at Ambient Temperatures, *Japanese J. Appl. Phys.*38, pp.L574-L576.

Liang, C. S and Wu, J. M. 2005. Electrical properties of W-doped $(Ba_{0.5}Sr_{0.5})TiO_3$ thin films, *J. Crys. Growth,* 274, pp.173-177.

Liu S, Li Y and Liu M. 2003. Crystallization behavior and ferroelectric properties of $PbTiO_3/Ba_{0.85}Sr_{0.15}TiO_3/PbTiO_3$ sandwich thin film on $Pt/Ti/SiO_2/Si$ substrates, *J. Electron. Mater.* 32, pp.1085-1089.

Mascot, M., Fasquelle, D. and Carru, J. C. 2011. Very high tunability of $BaSn_xTi_{1-x}O_3$ ferroelectric thin films deposited by sol-gel, *Funct. Mater. Lett*. 4, pp.49-52.

Piotrowski, J. and Roqalski, A. 1998. New generation of infrared photodetectors, Sensors and Actuators A: Physical. 67, pp.146-152.

Tsai, M. S, Sun, S. C and Tseng, T. Y. 1997. Effect of oxygen to argon ratio on properties of $(Ba,Sr)TiO_3$ thin films prepared by radio-frequency magnetron sputtering, *J. Appl. Phys.*82, pp.3482-3487.

Uchino, K. 1994. Relaxor ferroelectric devices, Ferroelectrics.151, pp.321-330.

Wang, H. W, Nien, S. W. and Lee, K. C. 2004. Enhanced tunability and electrical properties of barium strontium titanate thin films by gold doping in grains, *Appl. Phys. Lett*. 84, pp.2874-2876.

Yoon, K. H, Lee, J. C, Park, J, Kang, D. H, Song, C. M and Seu, Y. G. 2001. Electrical Properties of Mg Doped $(Ba_{0.5}Sr_{0.5})TiO_3$ Thin Films, *Japanese J. Appl. Phys.* 40, pp.5497-5500.

Zhang, T and Ni, H. 2002. Pyroelectric and dielectric properties of sol–gel derived barium–strontium–titanate $(Ba_{0.64}Sr_{0.36}TiO_3)$ thin films, Sensors and Actuators A: physical. 100, pp. 252-256.

****